12 March 1999

ELSEVIER

Chemical Physics Letters 302 (1999) 119–124

CHEMICAL PHYSICS LETTERS

Chemical dependence of interatomic X-ray transition energies and intensities – a study of Mn Kβ″ and $K\beta_{2,5}$ spectra

U. Bergmann [a], C.R. Horne [b], T.J. Collins [c], J.M. Workman [c], S.P. Cramer [a,d,*]

[a] *Physical Biosciences Division, Lawrence Berkeley National Laboratory, Berkeley, CA 94720, USA*
[b] *Environmental Energy Technologies Division, Lawrence Berkeley National Laboratory, Berkeley, CA 94720, USA*
[c] *Department of Chemistry, Carnegie Mellon University, Pittsburgh, PA 15213, USA*
[d] *Department of Applied Science, University of California, Davis, CA 95616, USA*

Received 22 September 1998; in final form 11 January 1999

Abstract

A study of ligand (N, O, F) 2s to metal (Mn) 1s 'interatomic' or 'crossover' X-ray transitions is reported. We show that the energy of the Kβ″ feature is related to the ligand 2s binding energy and can be used to identify the type of ligand. For oxygen-ligated Mn compounds, the strength of the Kβ″ transition decreases exponentially with increasing Mn–O distance. This can be used to predict distances to ~0.1 Å. The $K\beta_{2,5}$ energy shows shifts of ~1 eV per unit oxidation state. Kβ″ and $K\beta_{2,5}$ transitions are a promising tool for structural characterization of transition-metal complexes.

1. Introduction

A wide variety of X-ray spectroscopies require monochromatization of both incident and emitted radiation [1]. The development of extremely bright synchrotron radiation sources, combined with the introduction of more efficient emission spectrometers, has dramatically improved the sensitivity and quality of such experiments. This technical progress, along with improved theoretical understanding, has contributed to a surge of interest in X-ray fluorescence [2], X-ray Raman scattering [3], and their resonant counterparts – resonant inelastic X-ray emission or resonant X-ray scattering [4,5]. For example, soft X-ray resonance fluorescence has been used to monitor d–d and charge transfer excitations in transition-metal and rare-earth compounds such as MnO [6], CeO_2 [7], PrO_2 [8], and Cu-oxides [9]. Hard X-ray experiments have probed charge transfer excitations in NiO [10] and Nd_2CuO_4 [11] and quadrupolar transitions in Gd [12]. For the most part, the recent interest in X-ray emission has emphasized its use as a probe of electronic structure. In contrast, a large fraction of X-ray absorption experiments are devoted to unravelling molecular structure [13].

One contribution of high-resolution X-ray fluorescence to molecular structure determination has been in the area of 'site-selective X-ray absorption spectroscopy' [14]. Many problems in biological and materials science involve multiple species of a given element, and it is often difficult to decipher which X-ray absorption features arise from which components. If emission features unique to a single chemical species can be identified, they can be monitored

* Corresponding author. E-mail: spcramer@lbl.gov

0009-2614/99/$ - see front matter
PII: S0009-2614(99)00095-0

in a fluorescence-detected X-ray absorption measurement to provide site-selectivity. In previous work, we have demonstrated that chemical shifts in Mn $K\beta_{1,3}$ ($3p \rightarrow 1s$) fluorescence are large enough [2] to selectively record the XANES and EXAFS of different Mn oxidation states [14]. Spin state induced Fe $K\beta_{1,3}$ shifts also allowed site selective X-ray spectroscopy of Fe-porphyrins [15]. As part of a search for better chemical selectivity in fluorescence spectra, we have examined other parts of the Kβ spectra for a variety of Mn compounds.

Valence-to-core transitions are obvious candidates for chemically sensitive fluorescence lines, since the character of the valence orbitals changes the most between different chemical species. In first-row transition-metal spectra, the highest-energy valence-to-core transitions are generally referred to as the $K\beta_{2,5}$ region. These transitions fill the metal 1s vacancy from orbitals with metal 3d and/or 4p character along with ligand 2p or 3p character. At slightly lower energies are weak spectral features referred to as Kβ″ lines. For Mn complexes, previous work on these spectral regions has been reported by Koster and Mendel [16], by Urch [17], and by Mukoyama and co-workers [18,19]. In the present Letter we show that the energies of Kβ″ transitions can be used to identify the elemental type of ligand, while the intensities can be used to address the number and distance of neighboring ligands. The $K\beta_{2,5}$ region is shown to have large chemical shifts that can be used to identify oxidation states and facilitate site-selective EXAFS.

2. Experimental

2.1. Samples

MnO (99.5%) was obtained from Alfa/AESAR, MnF2, and $KMnO_4$ were from Aldrich Chemical, β-MnO_2 was from J.T. Baker, and $LiMn_2O_4$ was obtained from Chemetal, $[Et_4N][Mn(O)(\eta^4\text{-}L)]$ was prepared in the Collins lab as previously described [20,21]. $ZnMn_2O_4$ was made by calcining $ZnCO_3$ and $MnCO_3$ in air, first at 900°C for 24 h and then at 1050°C for 48 h. Li_2MnO_3 was prepared at Lawrence Berkeley National Laboratory by mixing Li_2CO_3 and $MnCO_3$ and calcining in air at 800°C. The compositions of $ZnMn_2O_4$ and Li_2MnO_3 sample were confirmed by X-ray powder diffraction. Mn(salen)N was synthesized by Chang, Low and Gray at Caltech [22].

2.2. The fluorescence spectrometer

The fluorescence spectrometer for these experiments employs eight 8.9 cm diameter Si(440) analyzer crystals operating at Bragg angles close to backscattering. Each crystal is glued to a spherically polished glass substrate to achieve a bending radius of 85 cm. The crystals were aligned on a Rowland circle with respect to sample and detector, and they captured a total solid angle of 0.07 sr. Numerous improvements compared to a previous design [23] have been accomplished. Most notably the employment of a He-filled bag that encloses the entire emitted beam path, more and larger crystals and a simplified scanning procedure. A detailed description of the instrument is available [24].

The energy resolution of the fluorescence spectrometer is mainly determined by the vertical size of the excitation beam. A well-defined excitation beam was obtained by placing a 1 mm vertical by 2 mm horizontal slit in front of the samples. The resulting energy resolution was between 0.7 eV (at 6470 eV) and 1.5 eV (at 6560 eV). The fluorescence intensity was measured with a NaI detector, using a Canberra model 1718 amplifier with 0.1 μs pulse shaping time. This detector was shielded with lead foil to reduce the background radiation (primarily from elastic scattering). A 3×15 mm entrance slit in the shielding allowed the fluorescence photons to reach the detector.

2.3. Data collection

The fluorescence experiments were performed at NSLS wiggler beamline X-25 [25] using a Si(111) double crystal monochromator and the vertical focusing mode. The samples were excited at 6700 eV with an incident energy resolution of ~ 2 eV, estimated by measuring the elastic scattering at 6470 eV. The incident flux (I_0) was recorded with an air-filled ion chamber, and the spectra were corrected for changes in I_0 resulting from ring current decay and monochromator heating. The incident beam intensity was

on the order of order 10^{12} photons/s. The samples were at room temperature during data collection.

The fluorescence spectra were taken in two regions. Near the strong $K\beta_{1,3}$ peak (below 6500 eV), the incident flux was reduced by beamline front end slits to keep the maximum count rate below 1.2×10^5 photons/s and hence assure a linear detector response. The collection time per point was 3 s in this region. For the weaker fluorescence features above 6500 eV, the full excitation beam intensity was used, and the data collection time was increased to 5 s per point. Typical step sizes were on the order of 0.2 eV, and the total acquisition time for each spectrum was $\sim$ 1 h.

3. Results and discussion

The general features of Mn K emission spectra are illustrated in Fig. 1, using MnF_2 data as a representative spectrum. The strongest emission comes from $K\alpha$ ($2p \rightarrow 1s$) transitions; $\sim$ 25% of the absorbed X-rays are emitted as $K\alpha$ fluorescence [26]. The next strongest feature is the $K\beta_{1,3}$ ($3p \rightarrow 1s$) region, often accompanied by a $K\beta'$ satellite. The $K\alpha$:$K\beta$ intensity ratio is on the order of 8:1 [19,27]. In the highest energy range appear the $K\beta_{2,5}$ features, which have been assigned as transitions from molecular orbitals with some Mn 4p character and as $3d \rightarrow 1s$ quadrupole transitions [16,17,28–30]. Intensity analysis of the $K\beta_{2,5}$ region is complicated by this mix of dipole and quadrupole character.

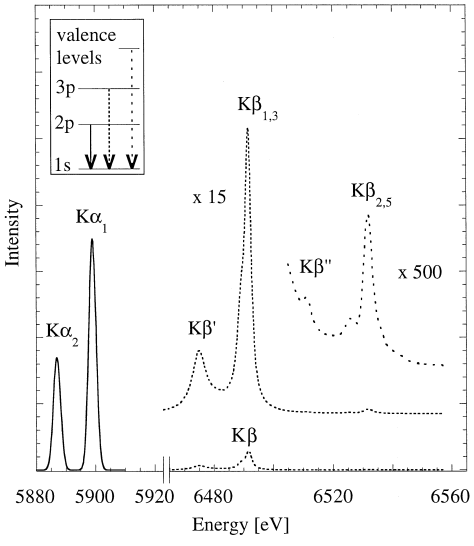

Fig. 1. K-emission spectrum of MnF2. The $K\alpha$ spectrum was simulated using the known $K\alpha/K\beta$ integrated intensity ratio of $\sim$ 7.7. The peaks $K\alpha_1$ and $K\alpha_2$ are a result of the spin–orbit interaction in the $2p^5$ core hole. The main $K\beta$ lines are split by the 3p–3d exchange interaction into a $K\beta_{1,3}$ peak and a $K\beta'$ feature. These are shown magnified by a factor 15 (dashed line). The much weaker $K\beta_{2,5}$ and $K\beta''$ features which are not visible in the main figure are shown magnified by a factor 500 (dotted line).

Below the $K\beta_{2,5}$ region at 6513 eV appears a peak referred to as $K\beta''$. The $1s \rightarrow 3d$ threshold energy is 6540 eV, hence the $K\beta''$ position indicates that an electron with a binding energy of $\sim$ 27 eV has fallen into the core hole. This value is close to the 2s binding energy of atomic F at $\sim$ 31 eV [31]. Best [28] as well as Jones and Urch [29] have assigned $K\beta''$ peaks observed in transition-metal oxides as ligand 2s to metal 1s 'interatomic' or 'crossover' transitions. They argue that the intensity of these transitions comes predominantly from mixing of metal 3p [28] or 3p and 4p [29] character with the ligand 2s orbitals. Mukoyama et al. have used $X\alpha$ calculations to quantitatively estimate crossover intensities; these calculations also suggest that most of the strength of the transitions comes from the metal character of the orbitals [19]. Since a large fraction of the electron density in the initial orbital is on the ligand, the 'interatomic' label still seems appropriate. To investigate these issues further, we have examined the $K\beta''$ spectra for a series of Mn complexes with different ligands as well as Mn–O complexes with different Mn–O bond lengths.

Fig. 2 shows the $K\beta$ spectra for a variety of Mn samples. A logarithmic scale is used to display the wide range of intensities. The relative strengths of the $K\beta_{1,3}$ and $K\beta''$ features above 6510 eV have been discussed previously [2]; they are characteristic of the 3p–3d exchange coupling. All of the oxygen-ligated Mn compounds exhibit $K\beta''$ transitions near 6520 eV. This $K\beta''$ transition is shifted to lower energies for the MnF_2 spectrum, and it is completely absent in the Mn metal spectrum. The energy of the $K\beta_{2,5}$ feature shifts $\sim$ 1 eV per increment in oxidation state (inset Fig. 2). Similar shifts in Mn spectra were observed by Koster and Mendel [16].

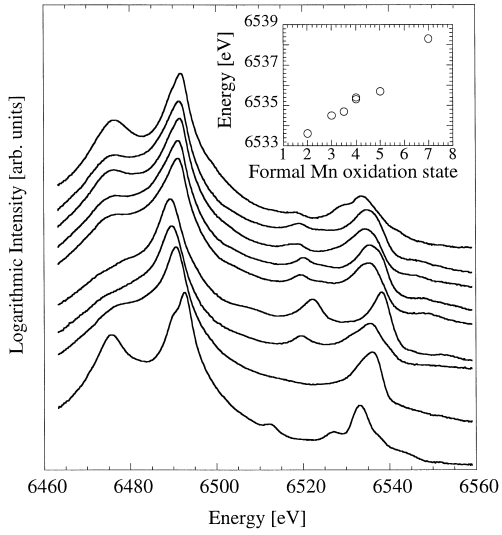

Fig. 2. Logarithmic intensity plot of Kβ spectra for a variety of Mn complexes. Top to bottom: $Mn^{II}O$, $LiMn^{III}Mn^{IV}O_4$, $ZnMn_2^{III}O_4$, $Li_2Mn^{IV}O_3$, β-$Mn^{IV}O_2$, $KMn^{VII}O_4$, $[Et_4N][Mn^{V}(O)(\eta^4\text{-L})]$, Mn metal, and MnF_2; (inset) $K\beta_{2,5}$ main peak energies as a function of Mn formal oxidation state.

To address the shifts of Kβ″ the spectra were further processed by aligning the peaks of the $K\beta_{2,5}$ lines. The remaining Kβ″ shifts should be related to the binding energy of the active electrons, modified slightly by any gap between filled and empty states and offset by a term related to the width of the $K\beta_{2,5}$. The resulting spectra (Fig. 3, top) show a variation of order 5 eV between adjacent Kβ″ energies for N, O, and F ligands and a total range of ~ 10 eV. The absolute energies increase with ligand atomic number, as expected for progressively deeper ligand 2s levels.

Interatomic transitions from many elemental types of ligands should be observable. The energies at which they occur should be a valuable diagnostic for the composition of the first coordination sphere. Because of the wide range of ligand 2s and 3s binding energies, Kβ″ transitions probably have the widest chemical shift range of any single transition-metal X-ray line.

When the spectra of different oxygen-ligated compounds are aligned to their $K\beta_{2,5}$ peak, there is little variation in the oxygen Kβ″ energies (Fig. 3, lower part). This is in agreement with XPS data for the two extreme cases MnO [32] and KMnO4 [33], which found O 2s energies of 21.6 and 22.1 eV, respectively. It indicates that the observed shifts in absolute Kβ″ energy among different oxygen-ligated samples (see Fig. 2) are primarily due to changes in the Mn 1s binding energies.

The intensities of the oxygen Kβ″ lines are extremely variable (Fig. 3, lower part). The integrated Kβ″ intensities can be normalized by the integrated intensity of the main Kβ region (6463–6505 eV) and furthermore by the number of oxygen ligands

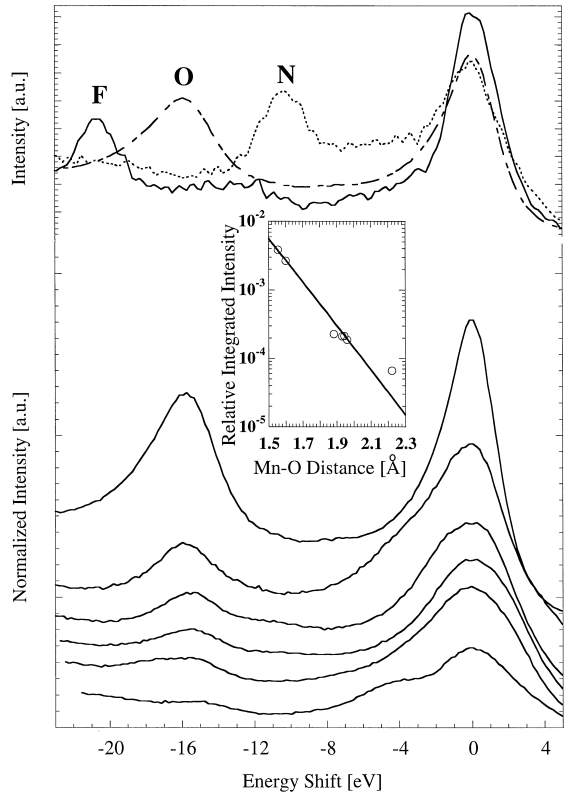

Fig. 3. (top) Kβ″ and $K\beta_{2,5}$ regions for samples with Mn–F, Mn–O, and Mn–N ligation. The energy zero has been shifted to put the main peak of the $K\beta_{2,5}$ line at 0 eV; (bottom) Kβ″ and $K\beta_{2,5}$ regions of Mn-oxides with different Mn oxidation states. Top to bottom: $KMn^{VII}O_4$, $[Et_4N][Mn^{V}(O)(\eta^4\text{-L})]$, β-$Mn^{IV}O_2$, $LiMn^{III}Mn^{IV}O_4$ and $ZnMn_2^{III}O_4$, $Mn^{II}O$, $Li_2Mn^{IV}O_3$. The intensities are normalized to the Kβ intensity in the region from 6463 to 6505 eV. (inset) Normalized intensities of Kβ″ as a function of Mn–O distance. The integrated normalized intensities as shown for some compounds at the bottom are further divided by the number of O-ligands per Mn to represent the interatomic transition probability per Mn–O pair. The solid line is the least-squares fit using an exponential type distance dependence.

per Mn. Assuming that the integrated intensity per Mn of the main Kβ region is chemically invariant, this procedure yields the relative Kβ″ transition probability per Mn–O pair. The normalized intensity falls almost exponentially as a function of the Mn–O distance (Fig. 3, inset). It is argued that the Kβ″ intensity derives primarily from the metal p character of the initial state wave function [28,29]. In perturbation theory the amount of metal p and ligand 2s mixing will depend on the overlap of these wave functions. Since they have exponential tails this overlap and hence the observed correlation between crossover intensity and bond length should vary exponentially with distance. It appears that the intensity of the Kβ″ line could be used as a tool to determine Mn–O distances to within ~ 0.1 Å.

4. Summary

We have studied the chemical sensitivity of the $K\beta_{2,5}$ and Kβ″ spectrum for a variety of Mn compounds. In favorable cases (short bond lengths), Kβ″ 'crossover' transitions from orbitals with a large amount of N, O, and F 2s character are clearly visible. The observed trends in fluorescence energies are in qualitative agreement with predictions from photo emission data, and different neighboring elements can easily be discriminated. Our study of Mn-oxides shows an intensity variation that is exponentially related to the Mn–O distance. Kβ″ spectroscopy, by itself or in conjunction with site-selective EXAFS, shows potential as a technique for determination of specific ligand types and distances.

Acknowledgements

This research was supported by the National Institutes of Health, grant GM-48145 (to SPC) and by the Department of Energy, Office of Health and Environmental Research. The National Synchrotron Light Source is supported by the Department of Energy, Office of Basic Energy Sciences. We thank H.B. Gray and C.J. Chang for generously providing the Mn(salen)N compound. We thank Dr. T. Richardson at LBNL for providing the $LiMn_2O_4$ sample. We are grateful to Dr. L.E. Berman and Dr. Z. Yin at NSLS for assistance in the use of beamline X-25.

References

[1] International Workshop on Raman Emission by X-ray Scattering, New Orleans, LA, 1995.
[2] G. Peng, F.M.F. De Groot, K. Hämäläinen, J.A. Moore, X. Wang, M.M. Grush, J.B. Hastings, D.P. Siddons, W.H. Armstrong, O.C. Mullins, S.P. Cramer, J. Am. Chem. Soc. 116 (1994) 2914.
[3] Y. Udagawa, N. Watanabe, H. Hayashi, J. Phys. (Paris) 7 (1997) 347.
[4] A. Kotani, J. Phys. (Paris) IV 7 (1997) 1.
[5] P.M. Platzman, E.D. Isaacs, Phys. Rev. B 57 (1998) 11107.
[6] S.M. Butorin, J.-H. Guo, M. Magnuson, P. Kuiper, J. Nordgren, Phys. Rev. B 54 (1996) 4405.
[7] S.M. Butorin, D.C. Mancini, J.-H. Guo, N. Wassdahl, J. Nordgren, J. Alloys Compounds 225 (1995) 230.
[8] S.M. Butorin, L.-C. Duda, J.-H. Guo, N. Wassdahl, J. Nordgren, J. Phys.: Condens. Matter 9 (1997) 8155.
[9] J.H. Guo, N. Wassdahl, P. Skytt, S.M. Butorin, Y. Ma, J. Nordgren, J. Phys. Chem. Solids 54 (1993) 1203.
[10] C.-C. Kao, W.A.L. Caliebe, J.B. Hastings, J.-M. Gillet, Phys. Rev. B 54 (1996) 16361.
[11] J.P. Hill, C.C. Kao, W.A.L. Caliebe, M. Matsubara, A. Kotani, J.L. Peng, R.L. Greene, Phys. Rev. Lett. 80 (1998) 4967.
[12] M.H. Krisch, C.C. Kao, F. Sette, W.A. Caliebe, K. Hämäläinen, J.B. Hastings, Phys. Rev. Lett. 74 (1995) 4931.
[13] D.C. Köningsberger, R. Prins (Eds.), X-ray Absorption, Principles, Applications, Techniques of EXAFS, SEXAFS, and XANES, Wiley, New York, 1988.
[14] M.M. Grush, G. Christou, K. Hämäläinen, S.P. Cramer, J. Am. Chem. Soc. 117 (1995) 5895.
[15] X. Wang, C.R. Randall, G. Peng, S.P. Cramer, Chem. Phys. Lett. 243 (1995) 469.
[16] A.S. Koster, H. Mendel, Phys. Chem. Solids 31 (1970) 2511.
[17] D.S. Urch, in: D.S. Urch (Ed.), X-ray Emission Spectroscopy, vol. 3, Academic Press, New York, 1979, p. 1.
[18] K. Mukoyama, K. Taniguchi, H. Adachi, Phys. Rev. B 34 (1986) 3710.
[19] T. Mukoyama, K. Taniguchi, H. Adachi, Phys. Rev. B 41 (1990) 8118.
[20] T.J. Collins, S.W. Gordon-Wylie, J. Am. Chem. Soc. 111 (1989) 4511.
[21] T.J. Collins, R.D. Powell, C. Slebodnick, E.S. Uffelman, J. Am. Chem. Soc. 112 (1990) 899.
[22] C.J. Chang, D.W. Low, H.B. Gray, Inorg. Chem. 36 (1997) 270.
[23] X. Wang, M.M. Grush, A.G. Froeschner, S.P. Cramer, J. Synth. Radiat. 4 (1997) 236.
[24] U. Bergmann, S.P. Cramer, SPIE (Soc. Photo-Opt. Instrum. Eng.) Proc. 3448 (1998) 198.
[25] L.E. Berman, J.B. Hastings, T. Oversluizen, M. Woodle, Rev. Sci. Instrum. 63 (1992) 428.

[26] M.O. Krause, J. Chem. Phys. Ref. Data 8 (1979) 307.
[27] S.I. Salem, S.L. Panossian, R.A. Krause, At. Data Nucl. Data Tables 14 (1974) 91.
[28] P.E. Best, Chem. Phys. 44 (1966) 3248.
[29] J.B. Jones, D.S. Urch, J. Chem. Soc., Dalton Trans. (1975) 1885.
[30] K. Tsutsumi, H. Nakamori, K. Ichikawa, Phys. Rev. B 13 (1976) 929.
[31] J.A. Bearden, A.F. Burr, Rev. Mod. Phys. 39 (1967) 125.
[32] B. Hermsmeier, J. Osterwalder, D.J. Friedman, B. Sinkovic, T. Tran, C.S. Fadley, Phys. Rev. B 42 (1990) 11895.
[33] M. Oku, Electron Spectrosc. Relat. Phenom. 74 (1995) 135.